processes

MDPI

Article

Using ANN and Combined Capacitive Sensors to Predict the Void Fraction for a Two-Phase Homogeneous Fluid Independent of the Liquid Phase Type

Tzu-Chia Chen [1,*], Seyed Mehdi Alizadeh [2], Abdullah K. Alanazi [3], John William Grimaldo Guerrero [4], Hala M. Abo-Dief [5], Ehsan Eftekhari-Zadeh [6,*] and Farhad Fouladinia [7]

1 College of Management and Design, Ming Chi University of Technology, New Taipei City 243303, Taiwan
2 Petroleum Engineering Department, Australian University, West Mishref 13015, Kuwait
3 Department of Chemistry, Faculty of Science, Taif University, P.O. Box 11099, Taif 21944, Saudi Arabia
4 Department of Energy, Universidad de la Costa, Barranquilla 080001, Colombia; jgrimald1@cuc.edu.co
5 Department of Science and Technology, University College-Ranyah, Taif University, P.O. Box 11099, Taif 21944, Saudi Arabia
6 Institute of Optics and Quantum Electronics, Abbe Center of Photonics, Friedrich Schiller University Jena, 07743 Jena, Germany
7 Faculty of Electrical and Computer Engineering, Rzeszow University of Technology, Powstancow Warszawy 12, 35-959 Rzeszow, Poland
* Correspondence: tzuchiachen1688@gmail.com (T.-C.C.); e.eftekharizadeh@uni-jena.de (E.E.-Z.)

Abstract: Measuring the void fraction of different multiphase flows in various fields such as gas, oil, chemical, and petrochemical industries is very important. Various methods exist for this purpose. Among these methods, the capacitive sensor has been widely used. The thing that affects the performance of capacitance sensors is fluid properties. For instance, density, pressure, and temperature can cause vast errors in the measurement of the void fraction. A routine calibration, which is very grueling, is one approach to tackling this issue. In the present investigation, an artificial neural network (ANN) was modeled to measure the gas percentage of a two-phase flow regardless of the liquid phase type and changes, without having to recalibrate. For this goal, a new combined capacitance-based sensor was designed. This combined sensor was simulated with COMSOL Multiphysics software. Five different liquids were simulated: oil, gasoil, gasoline, crude oil, and water. To estimate the gas percentage of a homogeneous two-phase fluid with a distinct type of liquid, data obtained from COMSOL Multiphysics were used as input to train a multilayer perceptron network (MLP). The proposed neural network was modeled in MATLAB software. Using the new and accurate metering system, the proposed MLP model could predict the void fraction with a mean absolute error (MAE) of 4.919.

Keywords: capacitance sensor; concave sensor; ring sensor; two-phase flow; homogenous regime; artificial neural network (ANN); void fraction measuring

Citation: Chen, T.-C.; Alizadeh, S.M.; Alanazi, A.K.; Grimaldo Guerrero, J.W.; Abo-Dief, H.M.; Eftekhari-Zadeh, E.; Fouladinia, F. Using ANN and Combined Capacitive Sensors to Predict the Void Fraction for a Two-Phase Homogeneous Fluid Independent of the Liquid Phase Type. *Processes* **2023**, *11*, 940. https://doi.org/10.3390/pr11030940

Academic Editor: Jingtao Wang

Received: 5 March 2023
Revised: 14 March 2023
Accepted: 17 March 2023
Published: 20 March 2023

1. Introduction

There are many different types of two-phase fluids in industries, for instance, oil–gas, oil–water, and water–air. These fluids can be found in a wide variety of industries such as chemical, petrochemical, oil, and gas [1]. Nowadays, one of the most remarkable issues in the mentioned fields is precisely predicting the void fraction through multi-phase fluids [2]. Some other things that flow metering of fluids is important to are also worth mentioning such as procedure control, financial metering, and repository management. Due to the inherent complexity of two-phase fluids, flow metering of this kind of fluid is an arduous task [3]. In order to measure the flow of each phase in pipelines through the common method, firstly, two mixed phases separate and then each one of them will be calculated. This method can cause a lot of problems, for example, it is time-consuming and,

of course, expensive [4]. Therefore, designing and manufacturing flow meters can come with a multitude of benefits such as detecting the type of flow and measuring the void fraction, all of which can be done without any interruption to the process [5,6]. The void fraction in a two-phase air (or gas)–liquid fluid can be determined by dividing the portion of the pipe containing air by the entire cross-section of the pipe. Various non-destructive methods are available to calculate the void fraction [5–11]. Capacitive sensors are a suitable method for measuring the void fraction because they do not require interruption of the process or separation of phases. Electrodes are a crucial component of capacitive sensors and their configuration is remarkable for precise measurement. The type of liquid inside the pipe is directly related to the electrode configuration and concave, ring and helix are the most popular configurations. Choosing the electrode configuration for more accurate measurement depends on the type of liquid inside the pipe. Previous studies have focused on the three distinct flow regimes of stratified, annular, and homogeneous within a two-phase fluid in a pipe. For example, the concave electrode was recommended for a two-phase liquid–liquid conductive fluid [12–17]. Li et al. [18] studied the measurement error of capacitive sensors. They found that homogeneous sensitivity can reduce this error. Further research has been conducted to ameliorate a configuration that ensures homogeneous sensitivity and the helical electrode was found to have the highest level of homogeneous sensitivity [19–21]. Tollefsen and his colleagues [21] investigated a two-phase oil–water blend and found that capacitive sensors, utilizing direct plate surfaces, had a limitation in their reliance on regime and distribution and precise results could only be obtained if the components were thoroughly blended. If the size of the bubbles was smaller than the volume of the substance, the resulting mixture was roughly homogeneous. Jaworek et al. [22] analyzed two-phase water–air flow using five different structures (e.g., helix, concave, and double ring) and found that the concave configuration had the highest sensitivity. Furthermore, previous studies have examined the sensitivity of capacitance sensors in various two-phase flows. In [23], it was observed that the concave configuration had the highest sensitivity in a two-phase flow, while the double-ring structure had the lowest sensitivity. Kendoush and Sarkis [24] investigated air–solid two-phase flow. They tested various electrodes and found that the concave electrode has the highest sensitivity. Sami and Abouelwafa [25] conducted experiments on non-conductive liquid–gas two-phase flow using six different capacitors and found that the helical electrode was the most sensitive in oil–gas two-phase flow. They also discovered that the concave electrode offered the most accuracy for the annular pattern. In a study conducted by Ahmed [26], a capacitive sensor was utilized to detect the void fraction and identify the flow regime in a two-phase air–oil fluid through a horizontal pipe. The sensitivity of the capacitive sensor was evaluated using both concave and ring electrodes, with the latter indicating greater sensitivity. This study also highlighted the impact of the configuration type on the measured response as a limitation to accurately determining the void fraction. Roshani et al. [27] compared the performance of two well-known sensors in the multi-phase flow metering industry: gamma-ray attenuation-based and capacitance-based sensors. The sensors were tested in an annular air–oil two-phase flow. The momentary sensitivity of the sensors was obtained in different void fractions, in which the concave capacitance-based sensor had better performance in void fractions of 0.8–1. Wang et al. [28] used three different sensors in their investigation: concave, double ring, and array sensors. They researched the performance of the gas percentage of a two-phase fluid and using the obtained data, the type of regime was predicted. Krupa and his coworkers [29] used a type of capacitance-based sensor (such as concave) to measure the gas percentage in small channels with diameters of less than 10 mm. The frequency deviation of a high-frequency oscillator was implemented to calculate the gas percentage in two-phase flow after the capacitance sensor was coupled to a resonant circuit with an inductance in parallel. In [30], He and Chen used a multi-wire capacitance probe to measure the void fraction in stratified gas–liquid flow. This device was based on the single-wire capacitance probe and was able to measure the average and the local gas percentage by measuring the water level at various

positions of the pipe. Artificial intelligence (AI) is one of the most common methods in the industrial sector [31]. ANN is a capable tool that has been widely utilized in various fields, such as electrical engineering and control engineering [32–45]. The things that affects the performance of capacitance sensors are fluid properties. For instance, density, pressure, and temperature can cause large errors in the measurement of the void fraction. One of the solutions to this issue is a periodic recalibration of the instrument, which can be grueling. With the help of the previous studies in this field, in this study, an attempt was made to present an accurate metering system to predict the amount of void fraction regardless of the type of liquid. For this purpose, a two-phase-flow homogenous regime in different void fractions was simulated using COMSOL Multiphysics software. By considering both capacitance-based sensors, concave and ring, on the two-phase flow and applying their outputs to an MLP neural network, it we tried to predict void percentages with high precision. In fact, improving the detecting system's precision and the combination of two different capacitance-based sensors are the main contributions of the present research. The main aim of this paper was to present a technique based on ANN for intelligent estimating of the gas percentage in the two-phase flow regardless of the liquid phase changes. To train the ANN, a data set was created using COMSOL Multiphysics software. A combined capacitance-based sensor was modeled. This sensor was made from two widely used sensors, concave and ring, which were connected together in series. Simulations were done for a homogenous pattern of two-phase flow with five various liquid phases (crude oil, oil, gasoil, gasoline, and water) and the void fraction ranged from 0 to 1 with a step of 0.05. To predict the gas percentage of a homogeneous two-phase fluid with a distinct type of liquid, data obtained from the COMSOL Multiphysics were given as input to train a multilayer perceptron network (MLP) which was modeled in MATLAB software. Using the new and accurate metering system, the proposed MLP model could predict the void fraction with a low mean absolute error.

2. Validation and Simulations

Three distinct flow regimes are commonly observed in oil, chemical and petrochemical industries: annular, stratified, and homogeneous. These are illustrated in Figure 1. In this paper, a homogeneous regime for a two-phase air–liquid fluid was investigated. This type of regime happens when air and liquid inside the pipe are entirely blended. To benchmark the COMSOL Multiphysics software, based on the validated simulated data in the authors' previous work [46], in which two widely used capacitance-based sensors, concave and ring, were designed and simulated, the results obtained from this software are valid. COMSOL Multiphysics is one of the most widely used software programs. This software utilizes the finite-element method (FEM) to provide a specific environment to simulate and analyze different branches such as chemical, electrical, and mechanical industries. During simulation, an air area is created because there are powerful electric fields that exist around the plates of the simulated capacitor. Since the electrical field depends on the inverse of distance cubically, the more the distance between electrodes increases, the more the electrical field decreases. This way, the surrounding electrical field which could grow indefinitely will be negligible, as variables that affect the electrical field are constant over time the stationary study is used. As mentioned previously, COMSOL Multiphysics software uses a finite-element method for simulating and producing the most precise results. There are several types of meshing and the mesh size was set to finer. COMSOL Multiphysics software utilizes a network of elements to simulate and solve the designed structure with the finite-element method. The finer mesh size results in decreasing the size of each element, so in this way, the software produces a more accurate result. The size of the different parts of the finer mesh size are given in Table 1. The maximum element size limits how big each mesh element can be, the minimum element size limits how small each mesh element can be, the maximum element growth rate limits the size difference of two contiguous mesh elements, and the curvature factor and the resolution of narrow areas limits how big a mesh element can be along a curved boundary and controls the number of

layers of mesh elements in narrow regions. The computer that was used had an i7 4510U CPU and 6GB of RAM.

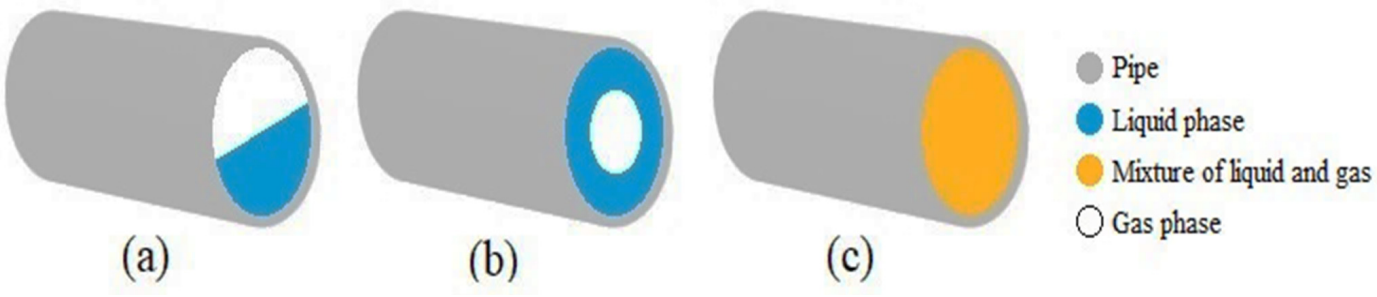

Figure 1. Distinct types of fluids. (**a**) Stratified, (**b**) annular, and (**c**) homogeneous.

Table 1. Characteristics of the finer mesh size.

Characteristics	Amount
The maximum element size	0.7 cm
The minimum element size	0.03 cm
The maximum element growth rate	1.35
The curvature factor	0.3
The resolution of narrow areas	0.85

2.1. Designing and Simulation of a Concave Sensor in COMSOL Multiphysics

In this section, the concave sensor was simulated in the benchmarked software. Simulations were performed for a two-phase air–liquid homogeneous fluid and every simulation was repeated 21 times (void fraction 0 to 1 with a step of 0.05) for five different liquids such as crude oil, oil, gasoil, gasoline, and water. The parameter by which the electric field between the charges is reduced in comparison to the vacuum is called relative permittivity (ε_r). To model the homogeneous pattern in the software, the material inside the pipe was assigned different values of ε_r. To achieve this, a specific ε_r was supposed for the interior material for each void fraction, obtained using an averaging method. The values of ε_r for air, crude oil, oil, gasoil, gasoline, and water at room temperature were 1, 2, 2.2, 2.4, 2.7, and 81, respectively. For example, for oil, the ε_r of the homogenous flow inside the pipe was incrementally changed from 1 to 2.2 for every 5% decrease in void fraction. In all of the simulations, air content was defined due to the obvious fringing fields that could be recognized around the capacitor plates. These fields might rise to infinite, even though they decrease inversely proportional to the cube of the distance. To account for this, a 3D model of electrostatic physics was made, with variables related to the field set to remain constant over time in the stationary regime. In addition, as was mentioned, the mesh settings for simulation were set on "finer mode". The simulated concave sensor with its dimensions is shown in Figure 2. A three-dimensional vision of the electrode schema, the meshed model of the capacitance-based sensor and the electrical potential (voltage) on the surf of the electrodes are illustrated in Figure 3. Moreover, fluid components were decomposed into 16429 3D fundamentals using FEM.

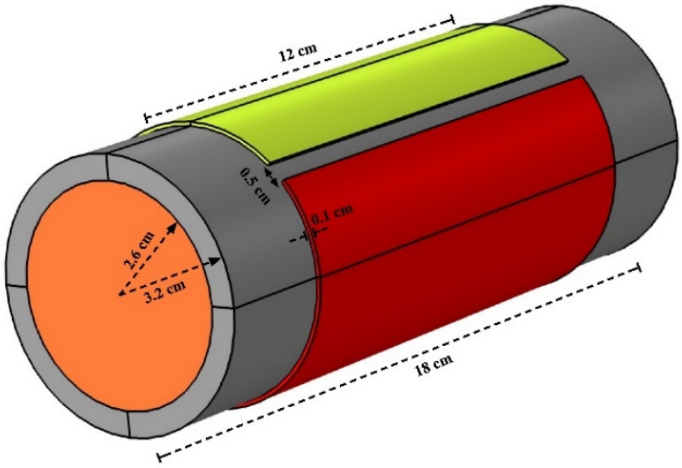

Figure 2. The simulated concave sensor in COMSOL Multiphysics.

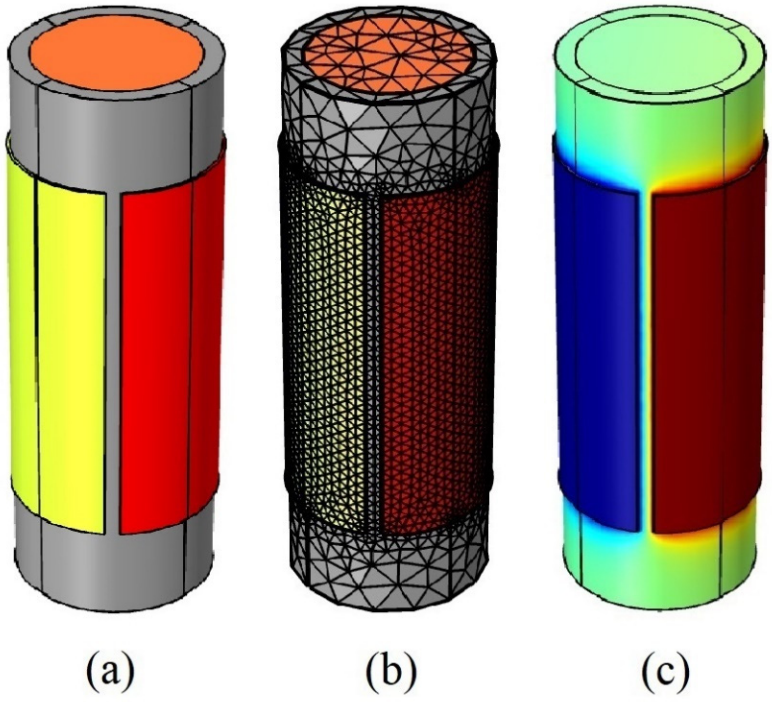

Figure 3. The simulated concave sensor. (**a**) Three-dimensional vision of the electrode schema, (**b**) meshed model, and (**c**) electrical potential (voltage) on the surf of the electrodes.

2.2. Designing and Simulation of a Ring Sensor in COMSOL Multiphysics

In this part, the ring sensor was simulated in the COMSOL Multiphysics software. All the mentioned things for the concave sensor were considered for this sensor as well. The simulated ring sensor is shown in Figure 4. In addition, as presented for the concave sensor, for the ring sensor, the three-dimensional vision of the electrode schema, the meshed model of the capacitance-based sensor and the electrical potential (voltage) on the surf of the electrodes are illustrated in Figure 5. Fluid components were decomposed into 16429 3D fundamentals using FEM. All of the results obtained from both sensors are presented in Table 2.

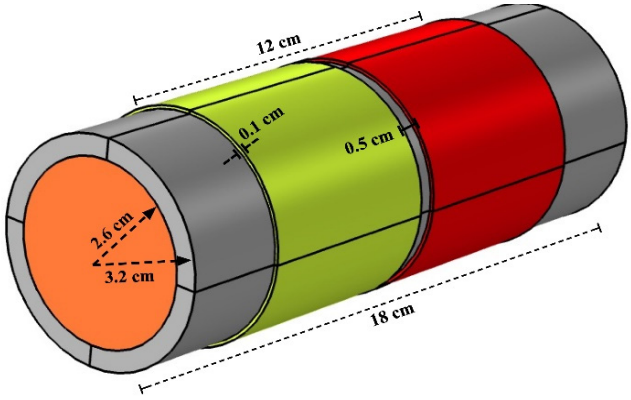

Figure 4. The simulated ring sensor in COMSOL Multiphysics.

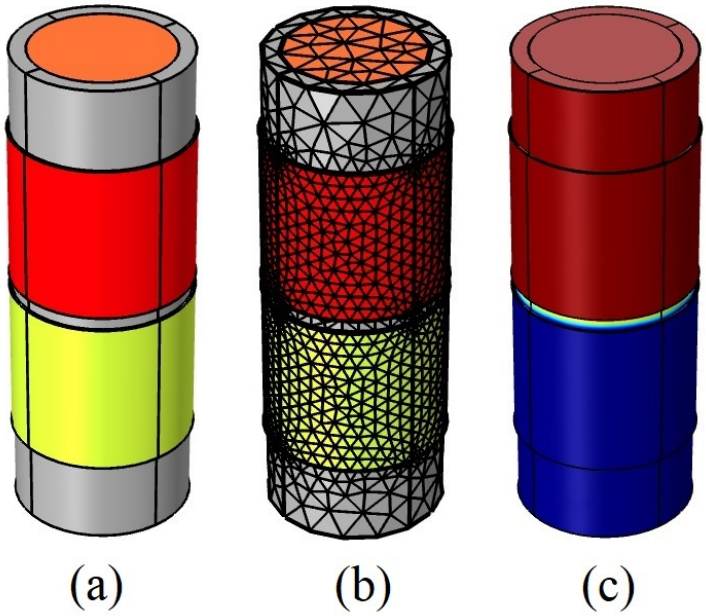

Figure 5. The simulated ring sensor. (**a**) Three-dimensional vision of the electrode schema, (**b**) meshed model, and (**c**) electrical potential (voltage) on the surf of the electrodes.

Table 2. The results obtained from simulating both sensors.

Liquid Phase Name	Void Fraction	ε_r	The Simulated Results of the Concave Sensor (pF)	The Simulated Results of the Ring Sensor (pF)
Crude oil	0.00	1.000	9.337	5.979
Crude oil	0.05	1.050	9.421	6.006
Crude oil	0.10	1.100	9.504	6.033
Crude oil	0.15	1.150	9.587	6.060
Crude oil	0.20	1.200	9.669	6.086
Crude oil	0.25	1.250	9.750	6.113
Crude oil	0.30	1.300	9.830	6.139
Crude oil	0.35	1.350	9.910	6.165
Crude oil	0.40	1.400	9.989	6.191
Crude oil	0.45	1.450	10.068	6.217

Table 2. *Cont.*

Liquid Phase Name	Void Fraction	ε_r	The Simulated Results of the Concave Sensor (pF)	The Simulated Results of the Ring Sensor (pF)
Crude oil	0.50	1.500	10.145	6.243
Crude oil	0.55	1.550	10.222	6.269
Crude oil	0.60	1.600	10.299	6.294
Crude oil	0.65	1.650	10.374	6.320
Crude oil	0.70	1.700	10.450	6.345
Crude oil	0.75	1.750	10.524	6.370
Crude oil	0.80	1.800	10.598	6.395
Crude oil	0.85	1.850	10.671	6.420
Crude oil	0.90	1.900	10.744	6.445
Crude oil	0.95	1.950	10.816	6.469
Crude oil	1.00	2.000	10.888	6.494
Oil	0.00	1.000	9.337	5.979
Oil	0.05	1.060	9.438	6.011
Oil	0.10	1.120	9.538	6.044
Oil	0.15	1.180	9.636	6.076
Oil	0.20	1.240	9.764	6.108
Oil	0.25	1.300	9.830	6.139
Oil	0.30	1.360	9.926	6.171
Oil	0.35	1.420	10.021	6.202
Oil	0.40	1.480	10.114	6.233
Oil	0.45	1.540	10.207	6.264
Oil	0.50	1.600	10.299	6.267
Oil	0.55	1.660	10.390	6.325
Oil	0.60	1.720	10.479	6.355
Oil	0.65	1.780	10.569	6.385
Oil	0.70	1.840	10.657	6.415
Oil	0.75	1.900	10.744	6.445
Oil	0.80	1.960	10.831	6.474
Oil	0.85	2.020	10.916	6.503
Oil	0.90	2.080	11.001	6.533
Oil	0.95	2.140	11.086	6.562
Oil	1.00	2.200	11.169	6.590
Gasoil	0.00	1.000	9.337	5.979
Gasoil	0.05	1.070	9.455	6.017
Gasoil	0.10	1.140	9.570	6.054
Gasoil	0.15	1.210	9.685	6.092
Gasoil	0.20	1.280	9.798	6.129
Gasoil	0.25	1.350	9.910	6.165
Gasoil	0.30	1.420	10.021	6.202
Gasoil	0.35	1.490	10.130	6.238

Table 2. *Cont.*

Liquid Phase Name	Void Fraction	ε_r	The Simulated Results of the Concave Sensor (pF)	The Simulated Results of the Ring Sensor (pF)
Gasoil	0.40	1.560	10.238	6.274
Gasoil	0.45	1.630	10.344	6.310
Gasoil	0.50	1.700	10.450	6.345
Gasoil	0.55	1.770	10.554	6.380
Gasoil	0.60	1.840	10.657	6.415
Gasoil	0.65	1.910	10.759	6.450
Gasoil	0.70	1.980	10.859	6.484
Gasoil	0.75	2.050	10.959	6.518
Gasoil	0.80	2.120	11.058	6.552
Gasoil	0.85	2.190	11.155	6.586
Gasoil	0.90	2.260	11.252	6.619
Gasoil	0.95	2.360	11.347	6.652
Gasoil	1.00	2.400	11.441	6.685
Gasoline	0.00	1.000	9.337	5.979
Gasoline	0.05	1.085	9.480	6.025
Gasoline	0.10	1.170	9.620	6.070
Gasoline	0.15	1.255	9.758	6.115
Gasoline	0.20	1.340	9.894	6.160
Gasoline	0.25	1.425	10.029	6.204
Gasoline	0.30	1.510	10.161	6.248
Gasoline	0.35	1.595	10.291	6.292
Gasoline	0.40	1.680	10.420	6.335
Gasoline	0.45	1.765	10.546	6.378
Gasoline	0.50	1.850	10.671	6.420
Gasoline	0.55	1.935	10.795	6.462
Gasoline	0.60	2.020	10.916	6.503
Gasoline	0.65	2.105	11.037	6.545
Gasoline	0.70	2.190	11.155	6.586
Gasoline	0.75	2.275	11.272	6.626
Gasoline	0.80	2.360	11.388	6.666
Gasoline	0.85	2.445	11.502	6.706
Gasoline	0.90	2.530	11.614	6.746
Gasoline	0.95	2.615	11.726	6.785
Gasoline	1.00	2.700	11.835	6.824
Water	0.00	1.000	9.337	5.979
Water	0.05	5.000	14.381	7.786
Water	0.10	9.000	17.492	9.162
Water	0.15	13.000	19.643	10.308
Water	0.20	17.000	21.226	11.300
Water	0.25	21.000	22.444	12.181

Table 2. *Cont.*

Liquid Phase Name	Void Fraction	ε_r	The Simulated Results of the Concave Sensor (pF)	The Simulated Results of the Ring Sensor (pF)
Water	0.30	25.000	23.411	12.973
Water	0.35	29.000	24.197	13.694
Water	0.40	33.000	24.849	14.355
Water	0.45	37.000	25.399	14.964
Water	0.50	41.000	25.869	15.529
Water	0.55	45.000	26.276	16.054
Water	0.60	49.000	26.631	16.544
Water	0.65	53.000	26.943	17.002
Water	0.70	57.000	27.221	17.433
Water	0.75	61.000	27.469	17.837
Water	0.80	65.000	27.692	18.219
Water	0.85	69.000	27.893	18.580
Water	0.90	73.000	28.077	18.921
Water	0.95	77.000	28.244	19.244
Water	1.00	81.000	28.397	19.551

As is clear from Table 2, there are 21 rows per liquid to consider the void fraction from 0 to 1 with a step of 0.05. In addition, for every specific liquid for the specific void fraction, the capacitance amount of both sensors was measured and considered.

3. Artificial Neural Network

Artificial intelligence (AI) has many applications across various industries such as healthcare, finance, retail, transportation, and education. AI can be used to analyze medical images, diagnose diseases, and personalize treatment plans. For example, AI-powered systems can help radiologists detect abnormalities in medical images and provide more accurate diagnoses as well as predict disease progression and develop personalized treatment plans for patients. It can also be utilized to detect fraud, optimize investment portfolios, and automate trading. This tool can analyze large amounts of financial data to identify patterns and anomalies that indicate fraudulent activity and optimize investment portfolios by identifying the most promising stocks and making trades automatically based on market conditions. It can also be used to personalize shopping experiences, recommend products, and optimize supply chain operations. AI can assist customers with their purchases and provide personalized product recommendations based on their preferences and past behavior. This tool is useful in optimizing supply chain operations by predicting demand, managing inventory levels, and optimizing shipping routes. Moreover, it can be used to improve safety, optimize traffic flow, and automated driving. For example, AI-powered systems can analyze traffic data to identify areas with high accident rates and develop solutions to reduce the risk of accidents. It can be utilized to personalize learning experiences, identify areas where students need help, and develop personalized learning plans. For example, AI-powered systems can analyze student performance data to identify areas where students are struggling and provide personalized learning materials to help them improve [47–51]. One of the most accurate methods in mathematics is ANN which consists of neurons. The ANN is a reliable soft computing approach that can address convoluted issues [52]. Neurons are simple computing elements and can be produced as one or more layers [53]. Classification and prediction are two important parts of ANN and because of this, many types of ANNs exist and each with its own characteristics. One of the best

ANNs with various applications is the multilayer perceptron (MLP). This makes it a good choice for researchers who need accurate results quickly [54]. This model has two sets of data, the training set and the testing set. A training set uses a finite amount of accurate data in order to train the network. A testing set consists of data that the network has never faced before and is defined with the aim of evaluating the network's correctness [55]. To find the appropriate network with the lowest mean absolute error, several networks with different characteristics such as the number of neurons, number of epochs, number of hidden layers, and even different types of activation functions have been investigated and the best one was chosen. In fact, after investigating different parts of networks and changing them over and over, the proposed network was selected. The modeled MLP network which can be seen in Figure 6 had a single output and two inputs. The capacitance obtained from the concave sensor and ring sensor was used as the first and second inputs, respectively. Table 1 displays the data obtained from the combined sensors for various liquids, including crude oil (ε_r = 2), oil (ε_r = 2.2), gasoil (ε_r = 2.4), gasoline (ε_r = 2.7), and water (ε_r = 81). Using COMSOL Multiphysics software, 105 simulations were conducted for the mentioned liquids by altering the void fractions from 0 to 1 with a step of 0.05. Out of these simulations, 73 (70%) were used as the train data and 32 (30%) were reserved for the test data. After evaluating multiple networks with various numbers of neurons and layers, the optimum structure was acquired. The characteristics of the modeled network are presented in Table 3.

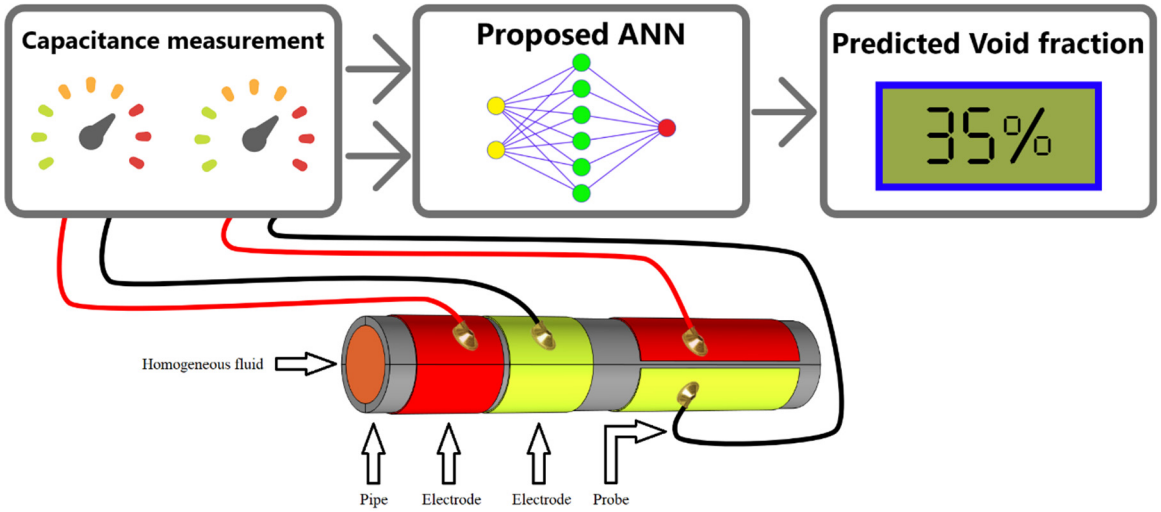

Figure 6. Diagram of predicting the void fraction using the proposed ANN.

Table 3. Configuration of the proposed ANN model.

Neural Network	**MLP**
Neurons in the input layer	2
Neurons in the hidden layer	6
Neurons in the output layer	1
Number of epochs	400
Activation function of neurons in hidden layers	Tansig
Activation function of neurons in input and output layers	Purelin
Method of training	Levenberg–Marquardt [56,57]

4. Results and Discussion

The diagram of predicting the void fraction using the proposed ANN is given in Figure 6. As mentioned previously, 105 sets of data were available from simulations and

70% and 30% of the data was used to train and to test, respectively. The data were divided randomly between the training and the testing sets. To opt for the best architecture many networks were investigated and the best one was chosen. There are two important factors in the results obtained from the presented ANN, real data and predicted data. Real data were produced by simulation and predicted data were provided by the proposed neural network; both are given in Figure 7. This figure shows that real and predicted data were close. By using Equation (1) the mean absolute error (MAE) of the proposed MLP model could be calculated. In this equation, N is the number of observations and X (Sim) and X (Pred) belong to simulated (COMSOL Multiphysics) and estimated (MLP) values, respectively. The regression diagrams of the training and testing data sets are shown in Figure 7a,b, respectively. Regression is a statistical technique that is used to evaluate the fortification of a relationship between two variables. MAE for the training and testing data sets were 4.621 and 4.919, respectively.

$$MAE = \frac{1}{N}\sum_{i=1}^{z}|x_i(Sim) - x_i(Pred)| \quad (1)$$

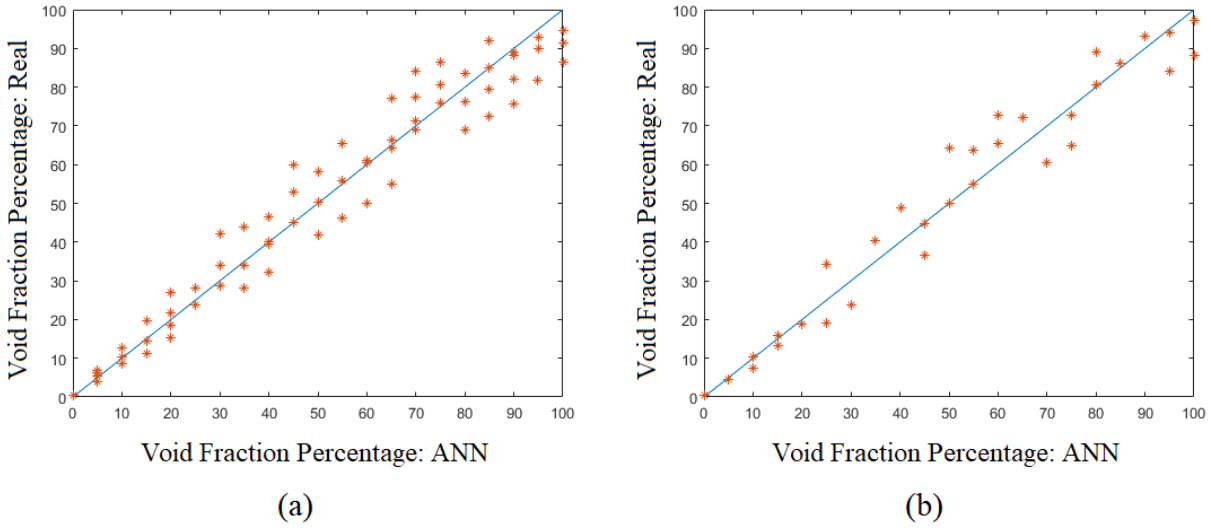

Figure 7. Regression diagrams of simulated and predicted results for (**a**) training set and (**b**) testing set.

Utilizing the accurate predicting system, the proposed MLP model can meter the void fraction with a low mean absolute error. This important point was achieved using an ANN and combined capacitive sensors. It is to be noted that the low MAE of the training and the testing sets show that the proposed ANN can give correct and accurate results. As can also be seen in Figure 7, underfitting or overfitting was not observed, which demonstrates the trustworthiness of the presented model. As mentioned previously, two different sorts of data are available for the ANN, training data and testing data. The network uses training data for training and creating the model and it contains information that is seen by the network. After training the modeled network is tested. At the end of calculating, the predicted values of training and testing data are compared with the real values of training and testing data. As can be seen, there is no over-fitting or under-fitting in the presented network.

5. Conclusions

The primary goal of this investigation was to predict the gas percentage of a two-phase fluid regardless of liquid phase changes. To achieve this aim, an MLP ANN was utilized. To supply data for the proposed ANN a new combined capacitance-based sensor was used. This sensor included a concave sensor and a ring sensor. Both of these sensors were designed and simulated in COMSOL Multiphysics software. Five different types of liquid were investigated: crude oil, oil, gasoil, gasoline, and water. Simulations were done

21 times (different void fractions ranging from 0 to 1 by a step of 0.05) for each liquid and this way 105 data sets were collected to train and test the modeled network. The presented ANN had two inputs (results obtained from the concave and ring sensors by simulating in COMSOL Multiphysics). This network also had one output which was the predicted void fraction. Applying the presented novel metering system, the gas percentage of any homogeneous two-phase flow with various liquid phases can be predicted accurately. In this regard, the functionality of an MLP ANN was investigated. The main aim was to predict the amount of void fraction precisely regardless of the type of liquid inside the pipe. To achieve this goal an MLP ANN and a combined capacitance-based sensor were used. Utilizing another type of ANN such as GMDH or RBF can be considered for future work. A combination of other shapes of sensors can also be considered.

Author Contributions: Methodology, T.-C.C., A.K.A., J.W.G.G., H.M.A.-D., F.F.; investigation, S.M.A., E.E.-Z., F.F. All authors have read and agreed to the published version of the manuscript.

Funding: This work was supported by the Taif University Researchers Supporting Project grant number (TURSP- 2020/266), of Taif University, Taif, Saudi Arabia. We acknowledge support from the German Research Foundation Projekt-Nr. 512648189 and the Open Access Publication Fund of the Thueringer Universitaets- und Landesbibliothek Jena.

Data Availability Statement: Not applicable.

Conflicts of Interest: The authors declare no conflict of interest.

References

1. Karimi, H.; Boostani, M. Heat transfer measurements for oil–water flow of different flow patterns in a horizontal pipe. *Exp. Therm. Fluid Sci.* **2016**, *75*, 35–42. [CrossRef]
2. Nazemi, E.; Roshani, G.H.; Feghhi, S.A.H.; Setayeshi, S.; Zadeh, E.E.; Fatehi, A. Optimization of a method for identifying the flow regime and measuring void fraction in a broad beam gamma-ray attenuation technique. *Int. J. Hydrogen Energy* **2016**, *41*, 7438–7444. [CrossRef]
3. Steven, R.N. Wet gas metering with a horizontally mounted Venturi meter. *Flow Meas. Instrum.* **2002**, *12*, 361–372. [CrossRef]
4. Wang, D.; Liang, F.; Peng, Z.; Wang, Y.; Lin, Z. Gas–liquid two-phase flow measurements by full stream batch sampling. *Int. J. Multiph. Flow* **2012**, *40*, 113–125. [CrossRef]
5. Banowski, M.; Beyer, M.; Szalinski, L.; Lucas, D.; Hampel, W. Comparative study of ultrafast X-ray tomography and wire-mesh sensors for vertical gas-liquid pipe flows. *Flow Meas. Instrum.* **2017**, *53*, 95–106. [CrossRef]
6. Salgado, C.M.; Dam, R.S.; Puertas, E.J.; Salgado, W.L. Calculation of volume fractions regardless scale deposition in the oil industry pipelines using feed-forward multilayer perceptron artificial neural network and MCNP6 code. *Appl. Radiat. Isot.* **2022**, *185*, 110215. [CrossRef] [PubMed]
7. Iliyasu, A.M.; Bagaudinovna, D.K.; Salama, A.S.; Roshani, G.H.; Hirota, K. A Methodology for Analysis and Prediction of Volume Fraction of Two-Phase Flow Using Particle Swarm Optimization and Group Method of Data Handling Neural Network. *Mathematics* **2023**, *11*, 916. [CrossRef]
8. Al-Lababidi, S.; Addali, A.; Yeung, H.; Mba, D.; Khan, F. Gas void fraction measurement in two-phase gas/liquid slug flow using acoustic emission technology. *J. Vib. Acoust.* **2009**, *131*, 501–507. [CrossRef]
9. Xie, C.G.; Stott, A.L.; Plaskowski, A.; Beck, M.S. Design of capacitance electrodes for concentration measurement of two-phase flow. *Meas. Sci. Technol.* **1990**, *1*, 65–78. [CrossRef]
10. Abdulkadir, M.; Hernandez-Perez, V.; Lowndes, I.S.; Azzopardi, B.J.; Brantson, E.T. Detailed analysis of phase distributions in a vertical riser using a wire mesh sensor (WMS). *Exp. Therm. Fluid Sci.* **2014**, *59*, 32–42. [CrossRef]
11. Koyama, S.; Lee, J.; Yonemoto, R. An investigation on void fraction of vapor–liquid two-phase flow for smooth and microfine tubes with R134a at adiabatic condition. *Int. J. Multiph. Flow* **2004**, *30*, 291–310. [CrossRef]
12. Demori, M.; Ferrari, V.; Strazza, D.; Poesio, P. A capacitive sensor system for the analysis of two-phase flows of oil and conductive water. *Sens. Actuators A Phys.* **2010**, *163*, 172–179. [CrossRef]
13. Strazza, D.; Demori, M.; Ferrari, V.; Poesio, P. Capacitance sensor for hold-up measurement in high-viscous-oil/conductive-water core-annular flows. *Flow Meas. Instrum.* **2011**, *22*, 360–369. [CrossRef]
14. An, Z.; Ningde, J.; Lusheng, Z.; Zhongke, G. Liquid holdup measurement in horizontal oil–water two-phase flow by using concave capacitance sensor. *Measurement* **2014**, *49*, 153–163. [CrossRef]
15. Ortiz, J.; Masek, V. Cyclonic capacitive sensor for multiphase composition measurement. *Sens. Transducers* **2015**, *191*, 1–11.
16. Zhai, L.S.; Jin, N.D.; Gao, Z.K.; Zhao, A.; Zhu, L. Cross-correlation velocity measurement of horizontal oil–water two-phase flow by using parallel–wire capacitance probe. *Exp. Therm. Fluid Sci.* **2014**, *53*, 277–289. [CrossRef]

17. Zhai, L.; Jin, N.; Gao, Z.; Wang, Z. Liquid holdup measurement with double helix capacitance sensor in horizontal oil–water two-phase flow pipes. *Chin. J. Chem. Eng.* **2015**, *23*, 268–275. [CrossRef]
18. Li, J.; Kong, M.; Xu, C.; Wang, S.; Fan, Y. An integrated instrumentation system for velocity, concentration and mass flow rate measurement of solid particles based on electrostatic and capacitance sensors. *Sensors* **2015**, *15*, 31023–31035. [CrossRef]
19. Elkow, K.J.; Rezkallah, K.S. Void fraction measurements in gas-liquid flows under 1-g and μ-g conditions using capacitance sensors. *Int. J. Multiph. Flow* **1997**, *23*, 815–829. [CrossRef]
20. Li, H.; Yang, D.; Cheng, M.X. Sensitivity analysis of capacitance sensor with helical shaped surface plates. *CIESC J.* **2011**, *62*, 2292–2297.
21. Tollefsen, J.; Hammer, E.A. Capacitance sensor design for reducing errors in phase concentration measurements. *Flow Meas. Instrum.* **1998**, *9*, 25–32. [CrossRef]
22. Jaworek, A.; Krupa, A. Gas/liquid ratio measurements by rf resonance capacitance sensor. *Sens. Actuators A Phys.* **2004**, *113*, 133–139. [CrossRef]
23. Dos Reis, E.; da Silva Cunha, D. Experimental study on different configurations of capacitive sensors for measuring the volumetric concentration in two-phase flows. *Flow Meas. Instrum.* **2014**, *37*, 127–134. [CrossRef]
24. Kendoush, A.A.; Sarkis, Z.A. Improving the accuracy of the capacitance method for void fraction measurement. *Exp. Therm. Fluid Sci.* **1995**, *11*, 321–326. [CrossRef]
25. Abouelwafa, M.S.; Kendall, E.J. The use of capacitance sensors for phase percentage determination in multiphase pipelines. *IEEE Trans. Instrum. Meas.* **1980**, *29*, 24–27. [CrossRef]
26. Ahmed, H. Capacitance sensors for void-fraction measurements and flow-pattern identification in air–oil two-phase flow. *IEEE Sens. J.* **2006**, *6*, 1153–1163. [CrossRef]
27. Roshani, M.; Phan, G.T.; Nazemi, E.; Eftekhari-Zadeh, E.; Phan, N.H.; Corniani, E.; Tran, H.N.; Duong, V.H.; Roshani, G.H. Performance comparison of capacitance-based flowmeter with gamma-ray attenuation-based two-phase flowmeter for determining volume fractions in an annular flow regime's component. *Eur. Phys. J. Plus* **2021**, *136*, 24–27. [CrossRef]
28. Wang, X.; Chen, Y.; Wang, B.; Tang, K.; Hu, H. Sectional void fraction measurement of gas-water two-phase flow by using a capacitive array sensor. *Flow Meas. Instrum.* **2020**, *74*, 101788. [CrossRef]
29. Krupa, A.; Lackowski, M.; Jaworek, A. Capacitance sensor for measuring void fraction in small channels. *Measurement* **2021**, *175*, 109046. [CrossRef]
30. He, D.; Chen, S.; Bai, B. Void fraction measurement of stratified gas-liquid flow based on multi-wire capacitance probe. *Exp. Therm. Fluid Sci.* **2019**, *102*, 61–73. [CrossRef]
31. Shahsavari, M.H.; Veisi, A.; Roshani, G.H.; Eftekhari-Zadeh, E.; Nazemi, E. An Experimental and Simulation Study for Comparison of the Sensitivity of Different Non-Destructive Capacitive Sensors in a Stratified Two-Phase Flow Regime. *Electronics* **2023**, *12*, 1284. [CrossRef]
32. Zych, M.; Petryka, L.; Kępiński, J.; Hanus, R.; Bujak, T.; Puskarczyk, E. Radioisotope investigations of compound two-phase flows in an open channel. *Flow Meas. Instrum.* **2014**, *35*, 11–15. [CrossRef]
33. Chen, X.; Zheng, J.; Jiang, J.; Peng, H.; Luo, Y.; Zhang, L. Numerical Simulation and Experimental Study of a Multistage Multiphase Separation System. *Separations* **2022**, *9*, 405. [CrossRef]
34. Rushd, S.; Gazder, U.; Qureshi, H.J.; Arifuzzaman, M. Advanced Machine Learning Applications to Viscous Oil-Water Multi-Phase Flow. *Appl. Sci.* **2022**, *12*, 4871. [CrossRef]
35. Veisi, A.; Shahsavari, M.H.; Roshani, G.H.; Eftekhari-Zadeh, E.; Nazemi, E. Experimental Study of Void Fraction Measurement Using a Capacitance-Based Sensor and ANN in Two-Phase Annular Regimes for Different Fluids. *Axioms* **2023**, *12*, 66. [CrossRef]
36. Ssebadduka, R.; Le, N.N.; Nguele, R.; Alade, O.; Sugai, Y. Artificial Neural Network Model Prediction of Bitumen/Light Oil Mixture Viscosity under Reservoir Temperature and Pressure Conditions as a Superior Alternative to Empirical Models. *Energies* **2021**, *14*, 8520. [CrossRef]
37. Mayet, A.M.; Nurgalieva, K.S.; Al-Qahtani, A.A.; Narozhnyy, I.M.; Alhashim, H.H.; Nazemi, E.; Indrupskiy, I.M. Proposing a high-precision petroleum pipeline monitoring system for identifying the type and amount of oil products using extraction of frequency characteristics and a MLP neural network. *Mathematics* **2022**, *10*, 2916. [CrossRef]
38. Artyukhov, A.V.; Isaev, A.A.; Drozdov, A.N.; Gorbyleva, Y.A.; Nurgalieva, K.S. The rod string loads variation during short-term annular gas extraction. *Energies* **2022**, *15*, 5045. [CrossRef]
39. Isaev, A.A.; Aliev, M.M.O.; Drozdov, A.N.; Gorbyleva, Y.A.; Nurgalieva, K.S. Improving the efficiency of curved wells' operation by means of progressive cavity pumps. *Energies* **2022**, *15*, 4259. [CrossRef]
40. Mayet, A.M.; Alizadeh, S.M.; Nurgalieva, K.S.; Hanus, R.; Nazemi, E.; Narozhnyy, I.M. Extraction of time-domain characteristics and selection of effective features using correlation analysis to increase the accuracy of petroleum fluid monitoring systems. *Energies* **2022**, *15*, 1986. [CrossRef]
41. Alanazi, A.K.; Alizadeh, S.M.; Nurgalieva, K.S.; Nesic, S.; Guerrero, J.W.G.; Abo-Dief, H.M.; Eftekhari-Zadeh, E.; Nazemi, E.; Narozhnyy, I.M. Application of neural network and time-domain feature extraction techniques for determining volumetric percentages and the type of two-phase flow regimes independent of scale layer thickness. *Appl. Sci.* **2022**, *12*, 1336. [CrossRef]
42. Roshani, M.; Phan, G.; Faraj, R.H.; Phan, N.H.; Roshani, G.H.; Nazemi, B.; Corniani, E.; Nazemi, E. Proposing a gamma radiation based intelligent system for simultaneous analyzing and detecting type and amount of petroleum by-products. *Nucl. Eng. Technol.* **2021**, *53*, 1277–1283. [CrossRef]

43. Roshani, G.H.; Hanus, R.; Khazaei, A.; Zych, M.; Nazemi, E.; Mosorov, V. Density and velocity determination for single-phase flow based on radiotracer technique and neural networks. *Flow Meas. Instrum.* **2018**, *61*, 9–14. [CrossRef]
44. Roshani, G.H.; Nazemi, E.; Roshani, M.M. Intelligent recognition of gas-oil-water three-phase flow regime and determination of volume fraction using radial basis function. *Flow Meas. Instrum.* **2017**, *54*, 39–45. [CrossRef]
45. Roshani, G.H.; Roshani, S.; Nazemi, E.; Roshani, S. Online measuring density of oil products in annular regime of gas-liquid two-phase flows. *Measurement* **2018**, 296–301. [CrossRef]
46. Iliyasu, A.M.; Fouladinia, F.; Salama, S.A.; Roshani, G.H.; Hirota, K. Intelligent Measurement of Void Fractions in Homogeneous Regime of Two-Phase Flows Independent of the Liquid Phase Density Changes. *Fractal Fract.* **2023**, *7*, 179. [CrossRef]
47. Esteva, A.; Robicquet, A.; Ramsundar, B.; Kuleshov, V.; DePristo, M.; Chou, K.; Cui, C.; Corrado, G.; Thrun, S.; Dean, J. A guide to deep learning in healthcare. *Nat. Med.* **2019**, *25*, 24–29. [CrossRef]
48. Li, J.; Yang, Z.; Li, W.; Li, Y. A survey on deep learning in finance. *Neural Comput. Appl.* **2020**, 3385–3407.
49. Rahimi, E.; Nguyen, T. Retail analytics: A review and future research directions. *J. Retail. Consum. Serv.* **2018**, 170–181.
50. Zhang, Z.; Liu, J.; Shen, Z.; Huang, J. A survey on deep learning for traffic prediction. *IEEE Trans. Intell. Transp. Syst.* **2019**, *99*, 3536–3553.
51. Kovanovic, V.; Joksimovic, S.; Gaševic, D.; Siemens, G.; Hatala, M. Applications of machine learning in education. *J. Educ. Technol. Soc.* **2018**, 33–47.
52. Rezvan, S.; Moradi, M.J.; Dabiri, H.; Daneshvar, K.; Karakouzian, M.; Farhangi, V. Application of Machine Learning to Predict the Mechanical Characteristics of Concrete Containing Recycled Plastic-Based Materials. *Appl. Sci.* **2023**, *13*, 2033. [CrossRef]
53. Roshani, G.; Feghhi, S.; Mahmoudi-Aznaveh, A.; Nazemi, E.; Adineh-Vand, A. Precise volume fraction prediction in oil–water–gas multiphase flows by means of gamma-ray attenuation and artificial neural networks using one detector. *Measurement* **2014**, *51*, 34–41. [CrossRef]
54. Gallant, A.R.; White, H. On learning the derivatives of an unknown mapping with multilayer feedforward networks. *Neural Netw.* **1992**, *5*, 129–138. [CrossRef]
55. Salgado, C.M.; Brandão, L.E.; Schirru, R.; Pereira, C.M.; da Silva, A.X.; Ramos, R. Prediction of volume fractions in three-phase flows using nuclear technique and artificial neural network. *Appl. Radiat. Isot.* **2009**, *67*, 1812–1818. [CrossRef]
56. Levenberg, K. A method for the solution of certain non-linear problems in least squares. *Q. Appl. Math.* **1944**, *2*, 164–168. [CrossRef]
57. Marquardt, D.W. An algorithm for least-squares estimation of nonlinear parameters. *J. Soc. Ind. Appl. Math.* **1963**, *11*, 431–441. [CrossRef]